Thermal valorisation of pulp mill sludge by co-processing with coal

R.N. Coimbra[a], *S. Paniagua*[a], *C. Escapa*[a], *L.F. Calvo*[a], *M. Otero*[a,b,1]

[a]Department of Applied Chemistry and Physics, IMARENABIO (Institute of Environment, Natural Resources and Biodiversity), Campus de Vegazana, University of León, 24071 León, Spain

[b]Department of Chemistry and CESAM (Centre for Environmental and Marine Studies), University of Aveiro, Campus de Santiago, 3810-193 Aveiro, Portugal

[1] Corresponding author: marta.otero@unileon.es; marta.otero@ua.pt

Abstract

The pulp and paper industry, which is a strategic economic sector in Europe, is very demanding in terms of energy and water. The high water consumption results in the generation of large volumes of wastewater, which must be treated to accomplish with regulations. Therefore, sludge is unavoidable generated and its management is a key issue for the pulp and paper industry. Given prohibitions on landfilling and land application, thermal co-processing with coal may be a viable management and valorisation option for such wastes. In this work, the separate combustion and pyrolysis of coal (C), primary (L1) and secondary (L2) pulp mill sludge and their respective blends (10 wt.% of either L1 or L2) was assessed by thermogravimetric (TG) analysis. Differential Thermogravimetric (DTG) curves made evident differences between C, L1 and L2, which were mainly related to the relative large fixed carbon and low volatiles content of C. However these differences, combustion of CL1 and CL2 mostly resemble that of C. Meanwhile, pyrolysis of CL1 and CL2 showed lower devolatilization temperatures and char yields, as compared with that of coal. Non-isothermal kinetic analysis evidenced only slightly lower apparent activation energy (E) for the combustion of C than for the combustion of either L1 or L2. Contrarily, much lower E were determined for the pyrolysis of CL1 and CL2 than for the pyrolysis of C. Yet, lower E than the weighted calculated ones where determined for the co-combustion and, especially, for the co-pyrolysis of the blends.

Keywords: thermal conversion; kinetics; Flynn-Wall-Ozawa; paper industry; wastes

1. Introduction

In Europe, the pulp and paper manufacturing and converting industries employ about 647.500 workers in 21.000 companies, generating an annual turnover of around 180 billion Euro [1]. As a counterpart, the pulp and paper industry is energy- and raw materials–intensive and considered one of the most polluting in the world [2]. Given the large water usage, huge volumes of wastewater are generated during various stages of pulping and papermaking activities [3]. In fact, this sort of industry is the third largest producer of wastewater after primary metals and chemicals industries [4].

In the pulp and paper industry, the main wastewater producing stages are wood preparation, pulp washing, pulp bleaching and paper making processes as well as the digester house [3]. At each stage, the wastewaters volume generated is closely related to the quantity of generated pulp in that particular process [5]. Depending on the type of applied processes, these wastewaters are characterized for having a high BOD content and various concentrations of other contaminants [3] so they can cause slime growth, thermal impacts, scum formation, color problems, and loss of aesthetic beauty in receiving waters [6]. They would also be a source of toxic substances in the aquatic environment, leading to the zooplankton and fish death, as well as profoundly affecting ecosystems [6]. Therefore, pulp and paper industry must treat effluents before discharging them into the environment in order to accomplish with environmental regulations [6]. Then, sludge is generated throughout primary and secondary wastewater treatment as a main end-product and must be treated before disposal [3]. In fact, handling, treatment and disposal of sludge produced from wastewater treatment represent an important percentage of total costs of pulp-and-paper industries [3, 7].

Given prohibitions on landfilling and since other alternatives such as agriculture application or composting are not viable due to the composition of sludge from the pulp

and paper industry, other management options must be undertaken. Nowadays, several waste recovery options may be considered for sludge from the pulp and paper industries, which include thermal processes such as combustion and/or, pyrolysis [7]. Ashes and char are the solid products of combustion and pyrolysis, respectively, which allow for an important reduction of volume of sludge from the pulp and paper industries [7]. Furthermore, valorisation of such wastes is possible by energy recovery by power and steam generation during combustion or by the production of gaseous or liquid fuels during pyrolysis [7,8]. On the other hand, and from an economic and practical point of view, the possibility of a joint processing of sludge from the pulp and paper industry with coal in existing plants may be an interesting option, since it allows for the use of existing infrastructures already equipped with appropriate devices for emission control, reducing at the same time fossil fuels consumption [9].

Thermogravimetric (TG) analysis has been widely employed for the study of the thermal processing of coal and different wastes, including those from the pulp and paper industry [10-15]. The main reason is that TG allows not only for a rapid assessment of the characteristic temperatures, maximum reactivity, or decomposition time, but also for assessing the process kinetics, reaction rates and activation energy [16]. In this work, the aim was to assess and compare the thermal behaviour during combustion and during pyrolysis of primary pulp mill sludge, secondary pulp mill sludge, a bituminous coal and their respective blends (10 wt.% of either primary or secondary pulp mill sludge). For this purpose, thermogravimetric analysis was carried out and the Flynn, Wall and Ozawa non-isothermal kinetic model was applied in order to determine the apparent activation energy associated to the single combustion and pyrolysis as well to that related to the co-combustion and co-pyrolysis of primary and secondary pulp mill sludge with coal.

2. Materials and methods

2.1. Materials

A bituminous coal (C) from the north coalfield of León (Spain) and commonly exploited in thermal power stations was used in this study. Both primary and secondary pulp mill sludge were provided by a mill that uses eucalyptus wood (*Eucalyptus globulus*) for the production of pulp by the kraft ECD (elemental chlorine free) process. At this mill, primary and secondary sludge are generated at an average rate of 20 and 10 kg per ton of air dried pulp produced, respectively. Primary sludge (L1) results from fibres rejected after the cooking/digestion at the pulping step, losses of fibres and other solids within liquid streams involved in the process (for example, washing and bleaching). The composition of the L1 is very similar to that of the pulp and basically consists of cellulosic fibres. Secondary sludge (L2) results from the clarification stage following the biological treatment to which wastewater is submitted after the primary clarification. During the biological treatment microorganisms are used to reduce the organic content of this wastewater. Essentially, secondary sludge is the resulting dehydrated biomass, including recalcitrant organic matter, e.g. lignocellulose residues.

C, L1 and L2 air dried samples were sieved so to have a 0.105 mm < particle diameter < 0.210 mm. Then, samples were characterized for heating value, proximate and elemental analysis and heating value. Higher heating value (HHV) at a constant volume was measured by means of an adiabatic oxygen bomb calorimeter. Proximate determinations were made according to modified procedures from ASTM D 3172 to D 3175 (Standard Practice for Proximate Analysis of Coal and Coke), E 870 (Standard Methods for Analysis of Wood Fuels), D 1102 (ash in wood) and E 872 (volatile matter). For the elemental determination, a LECO equipment model CHN-600 was used to determine the carbon, hydrogen and nitrogen content. Sulphur was determined by

means of a LECO model SC-132. Table 1 shows the HHV, proximate and elemental analysis of C, L1 and L2 [17].

2.2. Thermogravimetric analysis

Non-isothermal thermogravimetric analysis was carried out in a Setaram equipment, model SETSYS Evolution, which was calibrated (baseline, mass and temperature) prior utilization. Then, samples of C, L1 and L2 and their respective blends CL1 (containing 10 wt.% of L1) and CL2 (containing 10 wt.% L2) were submitted to dynamic runs, which were carried out up to 1200 K at a heating rate ($\beta = dT/dt$) of 0.5 K/s. Temperature-programmed combustion and pyrolysis runs were carried out under oxidizing and under inert atmosphere, respectively. Oxidizing atmosphere inside the furnace was obtained by means of a continuous airflow (100 cm^3/min) at a pressure of 1 atm (101 kPa). Inert atmosphere was provided by a continuous flow of N_2 (100 cm^3/min) at a pressure of 1 atm (101 kPa). For each sample and atmosphere, three repetitive TG curves were obtained in order to guarantee reproducibility of the results. All dynamic runs were carried out on a pan containing 25 ± 1 mg of the corresponding sample or blend.

In order to check interaction between C, L1 or L2 during co-combustion or co-pyrolysis, the theoretical DTG curves were calculated for each blend (CL1 and CL2) as a weighted average of the blend composition:

$$DTG_{CALCULATED} = 0.9 * DTG_{coal} + 0.1 * DTG_{sludge} \quad (1)$$

where DTG_{coal} is the mass loss rate of C and DTG_{sludge} is the mass loss rate of either L1 or L2.

2.3. Non-isothermal kinetic analysis

The rate of heterogeneous solid-state reactions can be generally described by:

$$\frac{\mathrm{d}\alpha}{\mathrm{d}t} = k(T)\, f(\alpha) \qquad (2)$$

where t is time, k(T) is the temperature-dependent constant and f(α) is a function called the reaction model, which describes the dependence of the reaction rate on the extent of reaction or fractional conversion, α.

The mathematical description of decomposition from a solid-state is commonly defined in terms of a kinetic triplet, as apparent activation energy, E, Arrhenius parameter, A, and an algebraic expression of the kinetic model in function of the fractional conversion f(α), which can be related to experimental data as follows:

$$\frac{\mathrm{d}\alpha}{\mathrm{d}t} = Ae^{-E/\mathrm{RT}} f(\alpha) \qquad (3)$$

Next, the above rate expression (2) can be converted into non-isothermal rate expressions describing reaction rates as a function of temperature at a constant heating rate, β:

$$\frac{\mathrm{d}\alpha}{\mathrm{d}T} = \frac{A}{\beta} Ae^{-\mathrm{E}/\mathrm{RT}} f(\alpha) \qquad (4)$$

Integrating up to conversion, α, Eq. (3) gives:

$$\int_0^{\alpha} \frac{\mathrm{d}\alpha}{f(\alpha)} = g(\alpha) = \frac{A}{\beta} \int_{T_0}^{T} e^{-E/\mathrm{RT}} \mathrm{d}T \qquad (5)$$

where g(α) is the integral kinetic function or integral reaction model when its form is mathematically defined.

Kinetic analysis is usually carried out to acquire an appropriate description of the process in terms of the apparent activation energy (E). Different methods may be used to analyse solid-state kinetic data [18], which may be classified according to the

selected experimental conditions and the performed mathematical analysis. Experimentally, either isothermal or non-isothermal methods are employed. Although the concepts of solid-state kinetics were established on the basis of isothermal experiments, the sample takes some time to reach the experimental temperature in this kind of experiments [18]. Non-isothermal experiments avoid this drawback. Mathematically, there are two possible approaches, the model-fitting and iso-conversional (model-free). Model-fitting methods were the first and most popular, especially for isothermal experiments, but they have lost popularity with respect to iso-conversional methods, which can compute kinetic parameters without modelling assumptions [19, 20]. Model-free isoconversional methods allow estimating the activation energy as a function of α without pre-fixing the reaction model. The essential assumption is that the reaction rate for a constant extent of conversion, α, depends only on the temperature [18].

In non-isothermal kinetics, several model-free isoconversional methods may be used. To use these methods, a series of experiments has to be conducted at different heating rates [21]. Among these methods, it is the one developed by Flynn, Wall and Ozawa [22,23] using the Doyle's approximation [24], which involves measuring the temperatures corresponding to fixed values of α from experiments at different heating rates. Furthermore, the Flynn-Wall-Ozawa method does not require the knowledge of the reaction order for the determination of the activation energy.

$$\ln(\beta) = \ln\left[\frac{AE}{Rg(\alpha)}\right] - 5.331 - 1.052\frac{E}{RT} \qquad (6)$$

To apply this method, it is necessary to obtain at least at three different heating rates (β), the respective conversion curves given by the measured TG data. Then, for each conversion value (α), plotting ln(β) versus. 1/T, gives a straight line with slope

−E/R, and thus the activation energy is obtained as a function of the conversion (α). Therefore, in this work, and in order to determine the activation energy of the combustion and pyrolysis of C, L1, L2 and their blends, thermogravimetric runs were carried out as described in the previous section (β= 0.5 K/s) at three more β: 0.1, 0.2 and 0.4 K/s.

3. Results and discussion

3.2. Thermogravimetric analysis

The DTG (Differential Thermogravimetric) results obtained from the temperature programmed combustion and pyrolysis of C, L1 and L2 at β = 0.5 K/s are shown in Figure 1, while those corresponding to their respective blends, CL1 and CL2, are shown in Figure 2. Also, weighted calculated DTG curves corresponding to the combustion and pyrolysis of the blends are shown in Figure 2 together with experimental curves.

On raising the temperature, combustion or the pyrolysis of the sample takes place with an associated weight loss. Then, when the fuel and/or volatiles content of the sample is exhausted, the mass, corresponding to the ashes or char remains stable in the combustion or pyrolysis DTG curves, respectively

In Figure 1, the combustion DTG curves corresponding to C 1 may be considered typical of a bituminous coal, the loss of volatiles and char gasification occurring in an only step, as for the large contribution of fixed carbon content in C (see Table 1) to the mass loss during combustion. Moreover, a slight weight gain due to oxygen chemisorption may be observed during the combustion of coal, which is not present in the DTG curves corresponding to L1 and L2. With respect to L1 and L2, their DTG combustion curves were different between them and also very different from C. In the case of L1, the weight loss during combustion occurred in two clear stages, which is

in agreement with results found by Yanfen et al. [13]. These authors [13] stated that the first and the second steps corresponded to the decomposition of combustible components and of mineral filling, respectively. The first stage must include the combustion of cellulose, which typically occurs at around 600K [13] while the second stage must be related to the combustion of calcium carbonate, which is characterized by burning at relative high temperatures. Regarding L2, four combustion steps may be observed throughout combustion, which are especially plain for the largest β used in this work (0.5 K/s). The first step, which is in the same temperature range than for L1, may be related to volatiles yield and combustion of cellulose [13,17]. Then, there is a shoulder that may be related to the combustion of biodegradable organics, probably generated during the wastewater biological treatment. The combustion of fixed carbon occurred next, in the same temperature range as for C. The last step, in the same temperature range as the second stage of the combustion of L1, must correspond to the decomposition of mineral content [13].

With respect to the pyrolysis DTG curves, it is evident that the mass loss associated to the pyrolysis of coal is very low compared to its combustion, as corresponds to the low volatiles content of coal (see Table 1). This is not the case of either L1 or L2, which pyrolysis DTG curves are more similar to their respective combustion profiles. Furthermore, weight loss during the pyrolysis of C occurs in an only step, while two steps are evident in the pyrolysis DTG curves of either L1 or L2. In any case, the pyrolysis DTG curves of L1 and L2 show plain peculiarities. As it may be seen in Figure 1 (see the scale of Y axis), more intense weight loss occurs during both steps of the pyrolysis of L1, as compared with L2, which is in agreement with the higher volatiles content of the first (see Table1). On the other hand, the first pyrolysis step occurs in a broader range of temperatures for L2 than for L1. In fact, the pyrolysis

DTG curve corresponding to L1 mostly resembles its combustion profile, which is in agreement with the low fixed carbon of L1 (see Table 1). However, for L2, the step corresponding to the combustion of fixed carbon is missed in its DTG pyrolysis curve while the shoulder corresponding to the second combustion step is still present in the pyrolysis curve. It may be said that differences between C and pulp mill sludge are relevant, but, there are also apparent differences between L1 and L2, either from a quantitative or qualitative point of view, as indicated by properties in Table 1 and DTG curves.

Experimental co-combustion curves in Figures 2 (a) and (b) mostly resemble the DTG combustion curve of C (Figure 1). However, it is to highlight the absence of the chemisorption weight gain, and moreover, in the case of CL1, remains the first step of the L1 combustion curve, which was associated to the combustion of the cellulosic content. Nevertheless, experimentally found differences corresponding to the first combustion step of CL1 and CL2 are less evident than the weighted calculated ones, as may be seen by DTG curves in Figures 2 (c) and (d). On the contrary, experimental co-pyrolysis curves in Figures 2 (a) and (b) are more different from the pyrolysis of coal than the weighted calculated curves in Figures 2 (c) and (d). These differences point to a synergetic effect of blending with L1 or L2, which stimulates volatilization of coal.

The characteristic parameters of the combustion and pyrolysis DTG experimental and calculated curves in Figure 1 and 2 are shown in Table 2. These parameters confirm the above said with respect to the corresponding curves. By comparing the characteristic parameters of DTG curves obtained under inert (pyrolysis) and oxidizing (combustion) atmosphere, differences are large for C, CL1 and CL2 but no less important for L1 and L2. It is also outstanding that the combustion of blends CL1 and CL2 resemble the combustion of C to a larger extent than in the case of

pyrolysis. Also, in the case of blends, combustion weighted calculated curves resemble the experimental ones largely than the pyrolysis weighted calculated curves resemble the corresponding experimental pyrolysis curves. Therefore, main interactions occurring between coal and L1 or L2 are due to their devolatilization, which must be related to the relative low volatiles content of coal as compared with L1 and L2 (see Table 1).

3.3. Non-isothermal kinetic analysis

The TG curves obtained from the temperature programmed combustion and pyrolysis of the single samples at the heating rates (β) of 0.1, 0.2, 0.4 and 0.5 K/s are depicted in Figure 3 together with the percentages of conversion considered for the kinetic analysis. In the same way, Figure 4 represents the TG combustion and pyrolysis curves corresponding to blends CL1 and CL2.

Curves in Figure 3 confirm large differences between weight loss during combustion and pyrolysis of C and similarities between these processes in the case of L1. Meanwhile, for L2, main differences between combustion and pyrolysis TG curves are related to the weight loss associated to the combustion of fixed carbon, which is absent in pyrolysis TG curves. In Figure 4, TG combustion curves corresponding to blends CL1 and CL2 mostly resemble those of C in Figure 3 (a). However, synergetic effects of blending are evidenced by the TG pyrolysis of CL1 and CL2, as compared with the pyrolysis curves of C (Figure 3 (d))

The plots of $ln\beta$ *vs.* $1/T$ corresponding to the several conversion degrees (α) considered for the combustion and pyrolysis are shown in Figure 5 for C, L1 and L2 and in Figure 6 for the blends CL1 and CL2. As it may be seen there is linearity for the several conversion percentages so, according with the Flynn–Wall–Ozawa kinetic

method [22-24], the activation energy E may be calculated from the corresponding slope.

Table 3 shows the E values determined for the combustion and pyrolysis of C, L1 and L2 and their respective blends CL1 and CL2. The average E determined for the combustion of coal C was 85 kJ/mol, while for L1 and L2 it was 155 and 199.4 kJ/mol, respectively. Differences between E values determined for the combustion of C, L1 and L2 are the same magnitude than those obtained for different rank coals [25]. Xie et al. [26], using the Flynn-Wall-Ozawa methods determined E values between 153 and 253 KJ/mol, which is a larger range than that of E here determined for L1 but lower than for L2. Also, in the literature, apparent activation energies determined by non-isothermal thermogravimetric for the combustion of biomass [27, 28] are mostly the same order than those here estimated for L1 and L2. Regarding the combustion of blends (10 wt.%), E values are both the same order as for the C combustion. However the average E determined for the combustion of L1 was lower than for the combustion of L2, in the blends with coal, the average E of the combustion of CL1 was higher than that of CL2. This is probable related to the large differences between the combustion profiles of C and L1, which did not show the fixed carbon combustion step. In any case, both for the combustion of CL1 and, especially, of CL2, the determined average E values were slightly lower than the weighted average calculated ones (92 and 96.4 KJ/mol, respectively).

The average E determined for the pyrolysis of C (255.6 KJ/mol) was quite higher than the one determined for the combustion (85 KJ/mol), and also higher than values determined for the pyrolysis of L1 (119.7 KJ/mol) and L2 (196.6 kJ/mol). In any case, the determined E values for the pyrolysis of C are similar to those found in the literature for coals [29]. No data were found in the literature on the pyrolysis of pulp

mill sludge, but it may be said that E values corresponding to the pyrolysis of L1 and L2 resemble those determined by other authors for the pyrolysis of lignocellulosic wastes [29]. Concerning the E determined for the pyrolysis of blends, the obtained values for CL1 (165.2 kJ/mol) and for CL2 (68.2 kJ/mol) are lower than the calculated weighted E that would correspond as proportional to the blends composition (246.6 and 249.7 KJ/mol, respectively). Differences, which are especially evident for CL2, hint that synergistic interactions may be occurring between C and L1 or L2 during their co-pyrolysis. This reduction could be related to coal interactions with cellulose, as highlighted by other authors [30,31], since lignocellulose must be an important constituent of L1 and L2.

Thermogravimetric results obtained in this work indicate that, under the appropriate conditions, co-processing of coal with primary and, especially, with secondary pulp mill sludge may be a management route for these wastes, which, furthermore, accounts with their valorisation. Moreover, it was confirm that TG analysis is very useful as a first and fast assessment tool for the consideration of thermal co-processing of wastes in existing infrastructures.

4. Conclusions

Large differences between C, L1 and L2 were plain by their respective DTG combustion and pyrolysis curves. These differences are mainly related to the higher fixed carbon and lower volatile content of C, as compared with L2 and, especially L1. However these differences, the combustion of blends CL1 and CL2, mostly resemble that of coal, except for the absence of the chemisorption and, in the case of CL1, also for the presence of the cellulose decomposition stage. Moreover, the apparent activation energy estimated for the co-combustion of C with L1 and L2 was slightly lower than that of coal. The pyrolysis DTG curve of C meant a very low weight loss, as compared

with L1 and L2, and was very different from the C combustion DTG curve. Then, the DTG pyrolysis curves of blends evidenced interactions between C and L1 or L2, which led to a higher devolatilization than the weighted calculated ones for CL1 and CL2. Globally, results obtained in this work showed the potential of thermal valorization of pulp mill sludge by co-processing with coal, which means an increase of coal reactivity and a decrease of the associated activation energy. In any case, from a practical point of view, for co-processing in existing plants, it must be taken into account the large volatiles content of L2 and, especially, of L1.

Acknowledgements

We would like to thank assistance given by María P. González Alonso and José A. de Linaje Aguirre, from LARECOM (Spain). Authors also thank the kind collaboration of Luís Machado and José Luís Amaral from RAIZ – Instituto de Investigação da Floresta e do Papel. FCT funding to the Associated Laboratory CESAM is acknowledged. C. Escapa acknowledges the Spanish Ministry of Education, Culture and Sports for her PhD fellowship (FPU12/03073). S. Paniagua acknowledges the grant for doctorate studies given by University of León in the framework of its own research program ULE-2014. Also, M. Otero acknowledges support from the Spanish Ministry of Economy and Competitiveness, State Secretariat for Research, Development and Innovation Spanish Ministry of Science and Innovation (RYC-2010-05634).

References

[1] European Comission: A blueprint for the EU forest-based industries (woodworking, furniture, pulp & paper manufacturing and converting, printing) http://eur-lex.europa.eu/legal-

content/EN/TXT/PDF/?uri=CELEX:52013SC0343&from=EN (2013). Last accessed on the 26th of May, 2015.

[2] Ince, B.K., Cetecioglu, Z., Ince, O.: Pollution Prevention in the Pulp and Paper Industries, Environmental Management in Practice, Dr. Elzbieta Broniewicz (Ed.), ISBN: 978-953-307-358-3, InTech, DOI: 10.5772/23709. Available from: http://www.intechopen.com/books/environmental-management-in-practice/pollution-prevention-in-the-pulp-and-paper-industries (2011). Last accessed on the 26th of May, 2015.

[3] Ashrafi, O., Yerushalmi, L., Haghighat, F.: Wastewater treatment in the pulp-and-paper industry: A review of treatment processes and the associated greenhouse gas emission. J. Env. Manage. (2015). doi: 10.1016/j.jenvman.2015.05.010

[4] Savant, D.V., Abdul-Rahman, R., Ranade, D.R.: Anaerobic degradation of adsorbable organic halides (AOX) from pulp and paper industry wastewater. Bioresour. Technol. 97, 1092-1104 (2006).

[5] The World Bank Group: Pollution prevention and abatement handbook, 1998: toward cleaner. The International Bank for Reconstruction and Development. Washington D.C., United states (1999).

[6] Pokhrel, D., Viraraghavan, T.:Treatment of pulp and paper mill wastewater-a review. Sci. Total Environ. 333, 37-58 (2004).

[7] Monte, M.C., Fuente, E., Blanco, A., Negro C.: Waste management from pulp and paper production in the European Union. Waste Manage. 29, 293–308 (2009).

[8] Elliott, A., Mahmood, T.: Survey benchmarks generation, management of solid residues. Pulp Pap. 79, 49–55 (2005).

[9] Vamvuka, D., Salpigidou, N., Kastanaki, E., Sfakiotakis, S.:Possibility of using paper sludge in co-firing applications. Fuel 88, 637–43 (2009).

[10] Otero M., Calvo L.F., Gil M.V., García A.I., Morán A.: Co-combustion of different sewage sludge and coal: a non-isothermal thermogravimetric kinetic analysis. Bioresource Technol. 99, 6311-6319 (2008).

[11] Sanchez, M.E., Otero, M., Gómez, X., Morán, A.: Thermogravimetric kinetic analysis of the combustion of biowastes. Renew. Energ. 34, 1622-1627 (2009).

[12] Liu, K., Ma, X.Q., Xiao, H.M.: Experimental and kinetic modeling of oxygen-enriched air combustion of paper mill sludge. Waste Manage. 30, 1206-1211 (2010).

[13] Yanfen, L., Xiaoqian, M.: Thermogravimetric analysis of the co-combustion of coal and paper mill sludge. Appl. Energ. 87, 3526–3532 (2010).

[14] Inguanzo, M., Domínguez, A., Menéndez, J.A., Blanco, C.G., Pis, J.J.: On the pyrolysis of sewage sludge: the influence of pyrolysis conditions on solid, liquid and gas fractions. J Anal Appl Pyrolysis. 63,209–222 (2002).

[15] Méndez, A., Fidalgo, J.M., Guerrero, F., Gasco, G.: Characterization and pyrolysis behaviour of different paper mill waste materials. J Anal Appl Pyrolysis 86, 66–73 (2009).

[16] Zhu, X., Chen, Z., Xiao, B., Hu, Z., Hu, M., Liu, C., Zhang, Q.: Co-pyrolysis behaviors and kinetics of sewage sludge and pine sawdust blends under non-isothermal conditions. J Thermal Anal Calorim. 119, 2269-2279 (2015).

[17] Coimbra, R.N., Paniagua, S., Escapa, C., Calvo, L.F., Otero, M.: Combustion of primary and secondary pulp mill sludge and their respective blends with

coal: a thermogravimetric assessment. Renew. Energ. (2015). doi: /10.1016/j.renene.2015.05.046

[18] Vyazovkin, S., Wight, C.A.: Isothermal and non-isothermal kinetics of thermally stimulated reactions of solids. Int Rev Phys Chem. 17, 407-33 (1998).

[19] Vyazovkin, S., Wight, C.A.: Model-free and model-fitting approaches to kinetic analysis of isothermal and nonisothermal data. Thermochim Acta 340–341, 53-68 (1999).

[20] Khawam, A., Flanagan, D.R.: Role of isoconversional methods in varying activation energies of solid-state kinetics: I. isothermal kinetic studies. Thermochim Acta 429, 93-102 (2005).

[21] Vyazovkin, S.: Evaluation of activation energy of thermally stimulated solid-state reactions under arbitrary variation of temperature. J Comput Chem. 18, 393-402 (1997).

[22] Ozawa, T.: A new method of analyzing thermogravimetric data. B. Chem. Soc. Jpn. 38, 1881-1886 (1965).

[23] Flynn, J.H., Wall, L.A.: A Quick, Direct method for the determination of activation energy from thermogravimetric data. Polym. Lett. 4, 323-328 (1966).

[24] Doyle, C.D.: Estimating isothermal life from thermogravimetric data. J. Appl. Polym. Sci. 6, 639-642 (1962).

[25] Kök, M.V.: Temperature-controlled combustion and kinetics of different rank coal samples. J. Therm. Anal. Calorim. 79, 175-180 (2005).

[26] Xie, Z., Ma, X.: The thermal behaviour of the co-combustion between paper sludge and rice straw. Bioresource Technol. 146, 611-618 (2013).

[27] Xiao, H.-m., Ma, X.-q., Lai, Z.-y.: Isoconversional kinetic analysis of co-combustion of sewage sludge with straw and coal. Appl. Energ. 86, 1741-1745 (2009).

[28] Idris, S.S., Rahman, N.A., Ismail, K.: Combustion characteristics of Malaysian oil palm biomass, sub-bituminous coal and their respective blends via thermogravimetric analysis (TGA). Bioresource Technol. 123, 581-591 (2012).

[29] Aboyade, A.O., Görgens, J.F., Carrier, M., Meyer, E.L., Knoetze, J.H.: Thermogravimetric study of the pyrolysis characteristics and kinetics of coal blends with corn and sugarcane residues. Fuel Processing Technol. 106, 310–320 (2013).

[30] Wu, Z., Wang, S., Zhao, J., Chen, L., Meng, H.: Synergistic effect on thermal behavior during co-pyrolysis of lignocellulosic biomass model components blend with bituminous coal. Bioresource Technol. 169, 220–28 (2014).

[31] Guo Z, Bai Z, Bai J, Wang Z, Li W. Synergistic effects during co-pyrolysis and liquefaction of biomass and lignite under syngas. J Therm Anal Calorim. 119, 2133-2140 (2015).

CAPTIONS TO FIGURES

Fig. 1 Combustion and pyrolysis DTG curves for C (a), L1 (b) and L2 (c). Note that the scale of figures has been adjusted for a better visualisation of DTG curves

Fig. 2 Experimental co-combustion and co-pyrolysis DTG curves for CL1 (a) and CL2 (b) and weighted average calculated co-combustion and co-pyrolysis DTG curves for CL1 (c) and CL2 (d)

Fig. 3 TG curves corresponding to the combustion of C (a), L1 (b) and L2 (c) and to the pyrolysis of C (d), L1 (e) and L2 (f) at different heating rates (β). The conversion percentages considered for kinetic analysis have been represented by straight lines crossing experimental data. Note that the scale of the Y axis has been adjusted for a better visualization of results.

Fig. 4 TG curves corresponding to the combustion of CL1 (a) and CL2 (b) and to the pyrolysis of CL1 (c) and CL2 (d) at different heating rates (β). The conversion percentages considered for kinetic analysis have been represented by straight lines crossing experimental data. Note that the scale of the Y axis has been adjusted for a better visualization of results.

Fig. 5 Fittings corresponding to the kinetic model proposed by Ozawa-Flynn-Wall to various conversion degrees (α) corresponding to the combustion of C (a), L1 (b) and L2 (c) and to the pyrolysis of C (d), L1 (e) and L2 (f). Note that the scales of axis have been adjusted for a better visualization of results.

Fig. 6 Fittings corresponding to the kinetic model proposed by Ozawa-Flynn-Wall to various conversion degrees (α) corresponding to the combustion of CL1 (a) and CL2 (b) and to the pyrolysis of CL1 (c) and CL2 (d). Note that the scales of axis have been adjusted for a better visualization of results.

Table 1. Proximate analysis, elementary analysis, and calorific values for the coal (C), the primary (L1) and the secondary (L2) pulp sludge used in combustion studies [17]

Properties	**C**	**L1**	**L2**
Proximate Analysis/ wt. %			
Moisture	11.22	1.74	11.83
Volatiles/ d.b.	8.01	65.25	58.64
Ashes	30.33	33.10	24.39
FC	61.66	1.65	16.97
Elemental Analysis/ wt. %, d.b.			
C	62.07	15.37	41.25
H	2.30	1.35	5.03
N	1.16	0.36	6.78
S	2.21	0.24	1.89
O*	1.93	49.58	20.66
Elemental Analysis / J/g, d.b.			
HHV	24382	2489	16429

FC = fixed carbon
HHV = high heat value
d.b. = dry basis
*calculated by difference

Table 2. Characteristic parameters obtained from the experimental DTG combustion and pyrolysis curves of coal (C), primary mill sludge (L1), secondary mill sludge (L2) and their respective blends with coal (CL1 and CL2)

Sample	Atmosphere	T_v	T_m	T_f	DTG_{max}	t_q
		(K)	(K)	(K)	(%/s)	(s)
C	Inert (pyrolysis)	620	964	1250	0.0097	1260
	Oxidizing (combustion)	649	915	1114	0.1162	930
L1	Inert (pyrolysis)	500	636	1090	0.3446	1180
	Oxidizing (combustion)	490	598	1077	0.6969	1174
L2	Inert (pyrolysis)	475	608	1150	0.1156	1350
	Oxidizing (combustion)	485	596	1030	0.1090	1090
CL1	Inert (pyrolysis)	500	637	1250	0.0269	1500
	Oxidizing (combustion)	529	923	1105	0.1097	1152
CL2	Inert (pyrolysis)	475	945	1250	0.0114	1550
	Oxidizing (combustion)	627	933	1100	0.1112	942
$CL1_{CALCULATED}$	Inert (pyrolysis)	500	635	1250	0.0341	1500
	Oxidizing (combustion)	530	910	1105	0.1048	1150
$CL2_{CALCULATED}$	Inert (pyrolysis)	475	605	1250	0.0114	1550
	Oxidizing (combustion)	505	900	1105	0.1128	1200

T_v = onset temperature for volatile release and weight loss

T_m = temperature of maximum weight loss rate

T_f = final pyrolysis of combustion temperature detected as weight stabilization.

DTG_{max} = maximum weight loss rate

t_q = combustion or pyrolysis time

Table 3. Apparent activation energy (E) estimated by the Flynn-Wall-Ozawa method for the combustion and pyrolysis of C, L1, L2 and their blends, at the considered conversion degrees (α)

Sample	α	Combustion		Pyrolysis	
		E (KJ/mol)	R^2	E (KJ/mol)	R^2
C	0.1	106.3	0.9995	195.1	0.9995
	0.2	99.5	0.9978	201.4	0.9978
	0.3	88.0	0.9882	199.9	0.9882
	0.4	78.7	0.9953	243.7	0.9953
	0.5	72.0	0.9864	329.8	0.9864
	0.6	65.8	0.9844	363.7	0.9844
		85.0*		**255.6***	
L1	0.1	160.9	0.9999	99.6	0.9999
	0.2	177.6	0.9742	96.6	0.9742
	0.3	135.1	0.9724	99.1	0.9724
	0.4	105.5	0.9986	103.1	0.9986
	0.5	163.0	0.9974	154.2	0.9974
	0.6	188.2	0.9935	165.7	0.9935
		155.0*		**119.7***	
L2	0.1	192.0	0.9694	113.5	0.9694
	0.2	209.9	0.9840	115.9	0.9840
	0.3	328.7	0.9315	173.7	0.9315
	0.4	194.8	0.9661	172.0	0.9661
	0.5	160.7	0.9880	259.6	0.9880
	0.6	110.6	0.9901	344.7	0.9901
		199.4*		**196.6***	
CL1	0.1	120.9	0.9874	201.9	0.9874
	0.2	99.7	0.9983	91.7	0.9983
	0.3	91.4	0.9737	140.0	0.9737
	0.4	86.9	0.9758	181.0	0.9758
	0.5	76.1	0.9704	229.8	0.9704
	0.6	69.6	0.9667	146.5	0.9667
		90.8*		**165.2***	
CL2	0.1	124.1	0.9873	56.6	0.9873
	0.2	94.4	0.9840	45.4	0.9840
	0.3	83.1	0.9640	53.1	0.9640
	0.4	79.1	0.9677	68.9	0.9677
	0.5	75.8	0.9729	93.9	0.9729
	0.6	69.6	0.9667	91.4	0.9667
		87.7*		**68.2***	

*calculated as arithmetic average of the E values determined for the different α

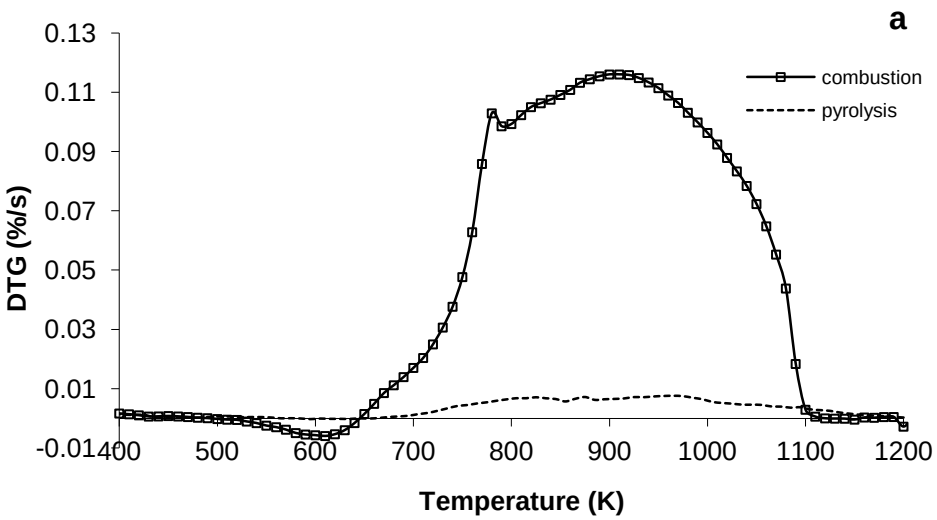
a
0.13
0.11
0.09
0.07
0.05
0.03
0.01
-0.01
DTG (%/s)
400
500
600
700
800
900
1000
1100
1200
Temperature (K)
combustion
pyrolysis

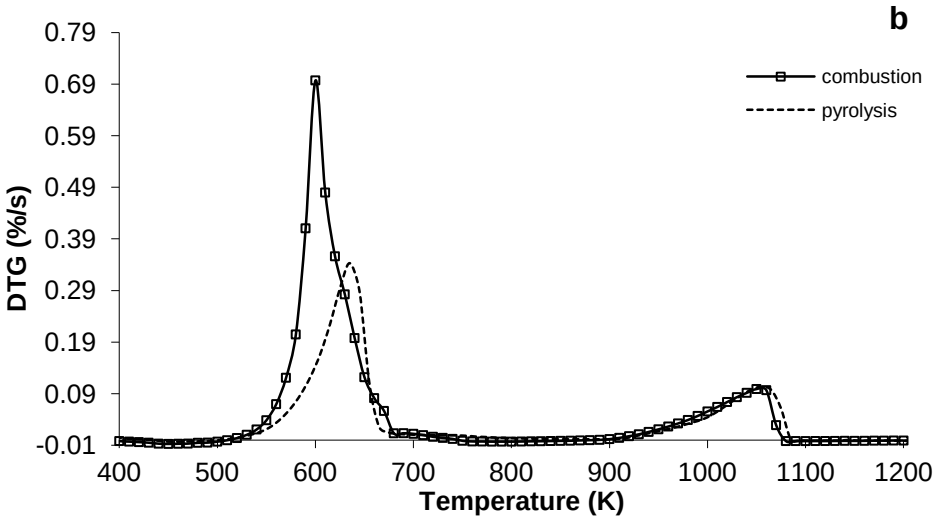
b
0.79
0.69
0.59
0.49
0.39
0.29
0.19
0.09
-0.01
DTG (%/s)
400
500
600
700
800
900
1000
1100
1200
Temperature (K)
combustion
pyrolysis

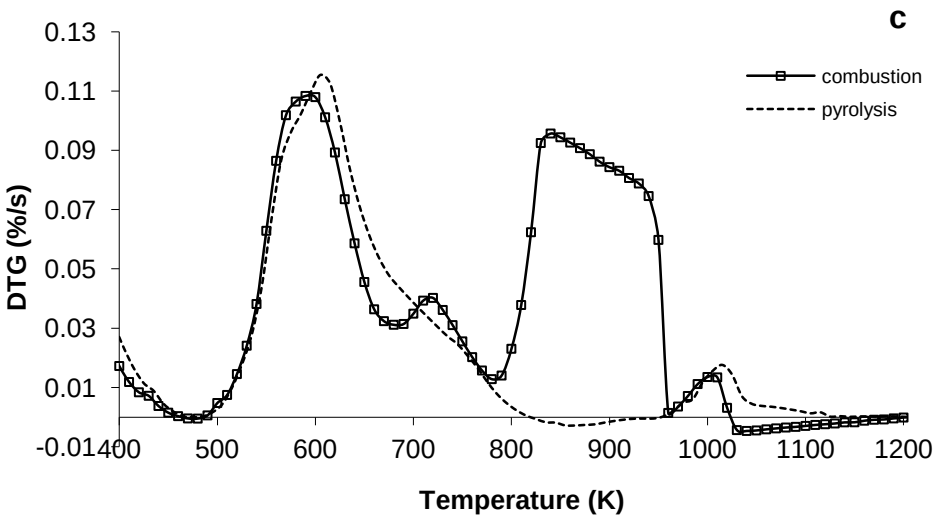
c
0.13
0.11
0.09
0.07
0.05
0.03
0.01
-0.01
DTG (%/s)
400
500
600
700
800
900
1000
1100
1200
Temperature (K)
combustion
pyrolysis

Fig. 1

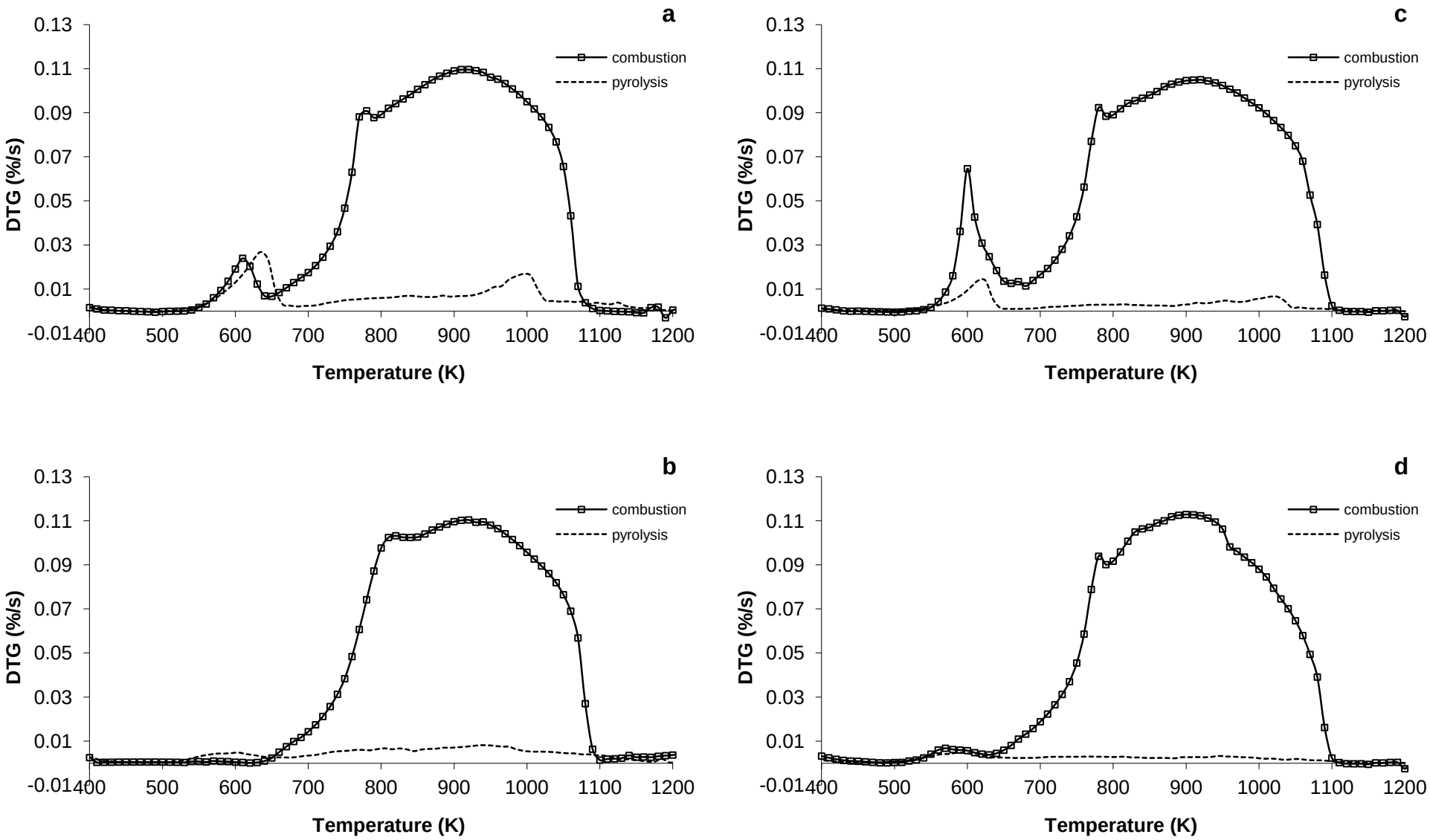
a
b
c
d
combustion
pyrolysis
DTG (%/s)
Temperature (K)
0.13
0.11
0.09
0.07
0.05
0.03
0.01
-0.01
400
500
600
700
800
900
1000
1100
1200

Fig. 2

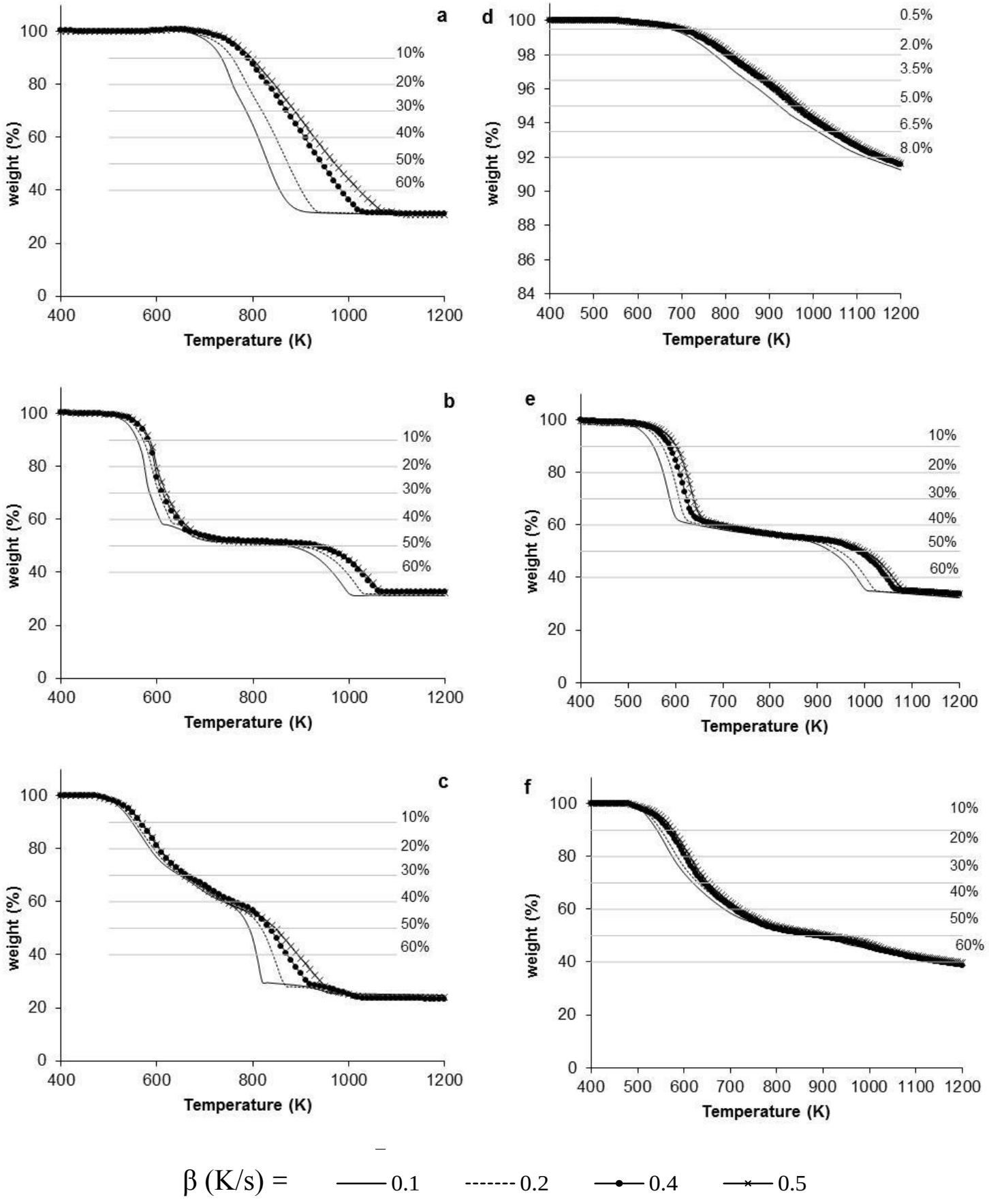
a
b
c
d
e
f
weight (%)
Temperature (K)
10%
20%
30%
40%
50%
60%
0.5%
2.0%
3.5%
5.0%
6.5%
8.0%
β (K/s) =
0.1
0.2
0.4
0.5

Fig. 3

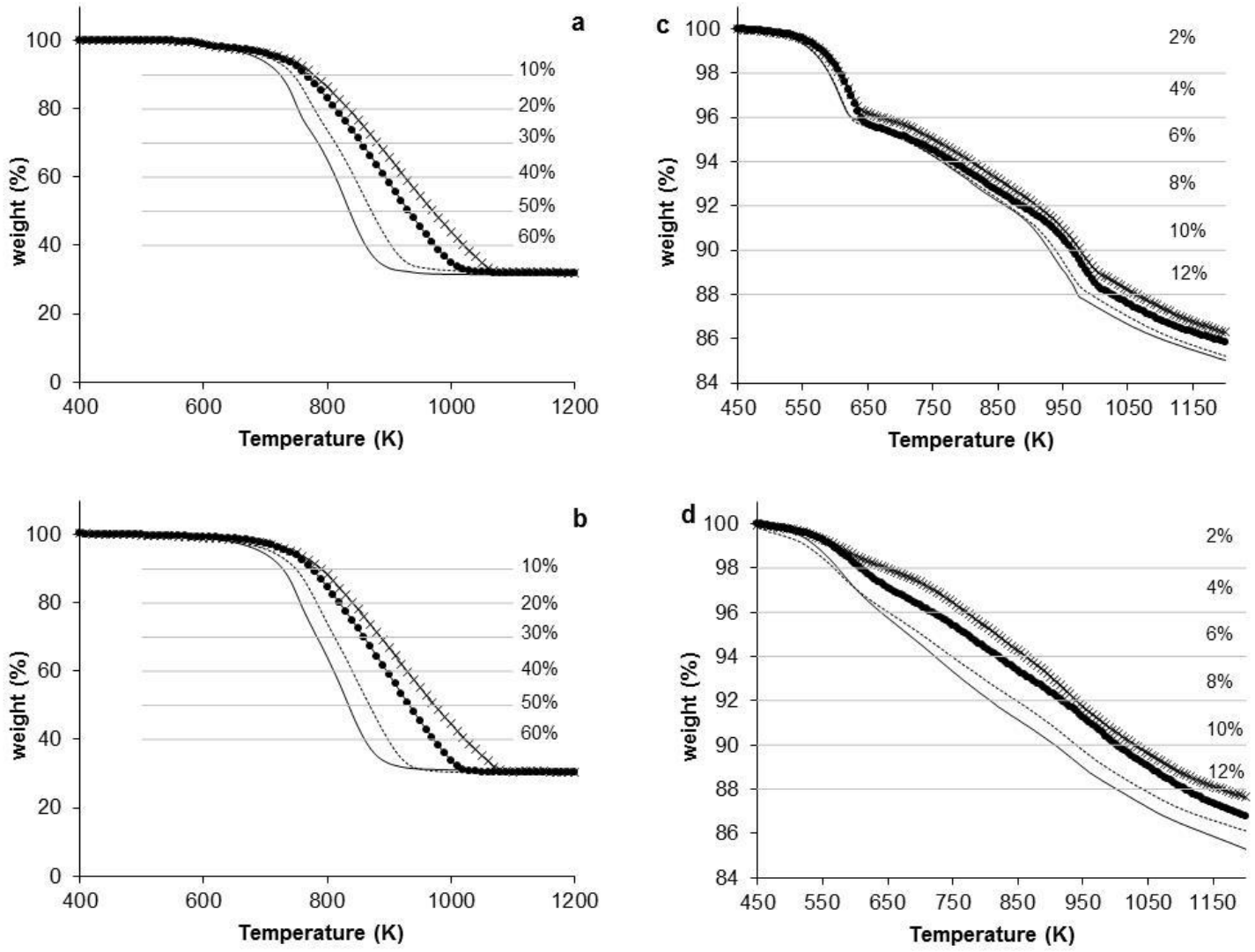
a
b
c
d
weight (%)
Temperature (K)
10%
20%
30%
40%
50%
60%
2%
4%
6%
8%
10%
12%
β (K/s) =
0.1
0.2
0.4
0.5

Fig. 4

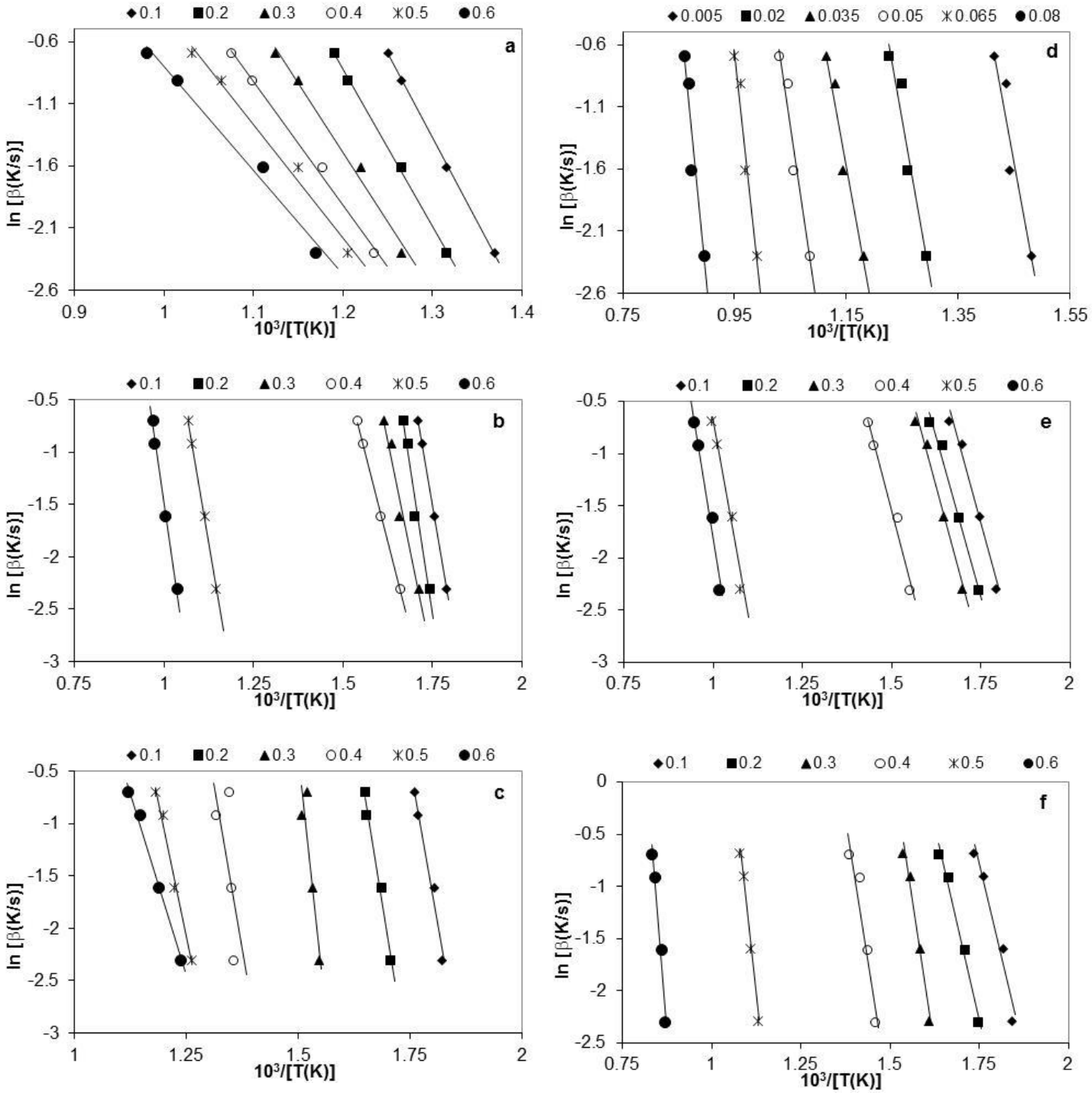

Fig. 5

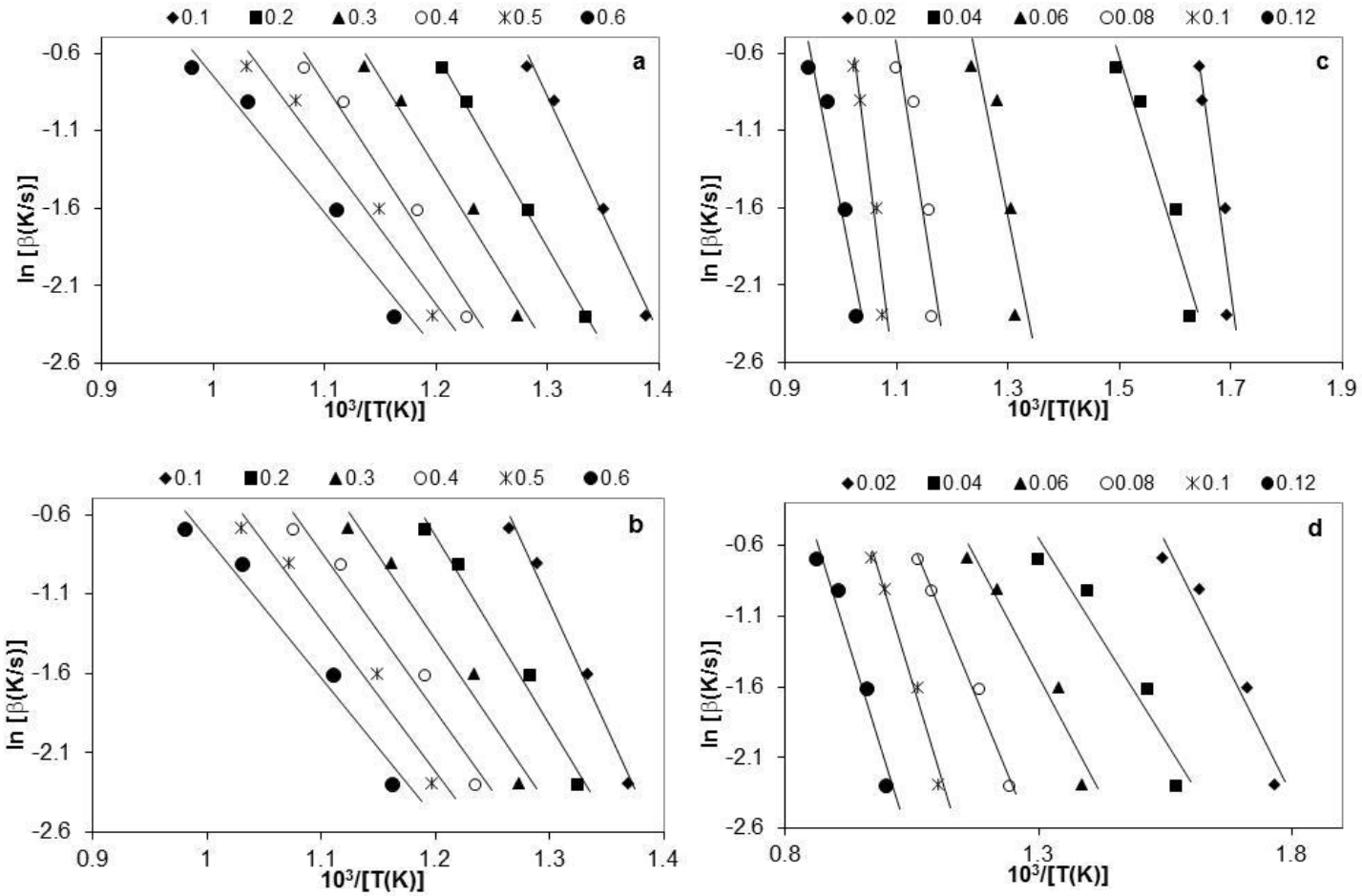

Fig. 6